



**SPECIAL ISSUE**

# Short light/dark cycles favour photosynthetic efficiency and growth in grapevines

Mariana Gómez Tournier<sup>1,2,3</sup>, Laurent Torregrosa<sup>1</sup>, Jana Kändler<sup>4</sup>, Angélique Christophe<sup>1</sup>, Romain Boulord<sup>1</sup>, Anna Medici<sup>5</sup>, and Anne Pellegrino<sup>1\*</sup>

<sup>1</sup> UMR LEPSE, Uni Montpellier, INRAE, Institut Agro, 2 place Pierre Viala, 34060 Montpellier, France

<sup>2</sup> Instituto Nacional de Tecnología Agropecuaria (INTA), Estación Experimental Agropecuaria (EEA) Mendoza, San Martín 3853, Luján de Cuyo, Mendoza 5507, Argentina

<sup>3</sup> Consejo Nacional de Investigaciones Científicas y Técnicas (CONICET) Mendoza, Av. Ruiz Leal s/n - Parque Gral. San Martín, Mendoza 5500, Argentina

<sup>4</sup> Pôle Vigne et Vin, Institut Agro, 2 place Pierre Viala, 34060 Montpellier, France

<sup>5</sup> UMR IPSIM, Uni Montpellier, CNRS, INRAE, Institut Agro, 2 place Pierre Viala, 34060 Montpellier, France

► This article is an (type d'article) published in cooperation with the 23rd GiESCO International Conference, July 21-27, 2025, hosted by the Hochschule Geisenheim University in Geisenheim, Germany.

Guest editors: Laurent Torregrosa and Susanne Tittmann.

**Article number: 9274**



\*correspondence:

anne.pellegrino@supagro.fr

Associate editor:

Susanne Tittmann



Received:  
5 March 2025

Accepted:  
30 June 2025

Published:  
18 July 2025



This article is published under the **Creative Commons licence (CC BY 4.0)**.

Use of all or part of the content of this article must mention the authors, the year of publication, the title, the name of the journal, the volume, the pages and the DOI in compliance with the information given above.

## ABSTRACT

Climate change and the expansion of the urban frontier pose a threat to the sustainability of agricultural systems. In this context, confined cultivation systems can provide a viable alternative for maintaining consistent production levels. Light and temperature in greenhouses or growth chambers are major regulatory factors in plant functioning, which can be easily modulated. Shortening the photo-/nycti-periods, compared to the standard cycle (12 h light/12 h dark), has been shown to enhance the photosynthetic activity and growth in annual crops, but its effect on perennial crops such as grapevines remains unexplored. This study aimed to describe the effects of accelerating the light/dark cycle to a repeated short pattern (3 h light/3 h dark, 'T3/3'), in contrast to the circadian-aligned regime (12 h light/12 h dark, 'T12/12') while keeping the same temperature and photosynthetic active radiation amounts per day. We evaluated photosynthetic efficiency, leaf growth, biomass production and partitioning, and resource use efficiency (water and light).

T3/3 in both genotypes maintained stable net photosynthetic rates (An) and high photosystem II efficiency ( $\phi$ PSII) during the light cycle, avoiding the 62 % drop observed under T12/12 after 3 h of exposure. In addition, the dark respiration (Rd) was reduced for T3/3 (–51 %) compared to T12/12, leading to a higher daily carbon gain (+66 %) for T3/3. Short light/dark cycle also increased total leaf area (LA) in both genotypes, due to a higher initial rate of leaf expansion (+52 %), and extended the duration of the vegetative phase (P1) by seven days compared to T12/12. However, the duration of the ripening period (P2) and total dry mass (DMtotal) did not show any differences between treatments and were mainly determined by genotypic variability. GENOT 102 showed a tendency to prioritise biomass partitioning to the reproductive organ and also produced more DMtotal (+38 %) compared to GENOT 16. Lastly, the efficiency in the use of resources (light and water) over the cycle was similar, regardless of the treatments and genotypes. These findings lay the foundation for adjusting light/dark cycles and genotype selection to maximise productivity and sustainability in confined growing environments.

**KEYWORDS:** plant physiology, circadian cycle, PAR, light use efficiency, biomass, GiESCO 2025

## INTRODUCTION

Climate change has a significant impact on agriculture, affecting water availability and increasing evapotranspiration (Bhatt & Hossain, 2019; Masia *et al.*, 2021). The need to maintain sufficient yield is thus coupled with the challenge of sustaining water resources (Malhi *et al.*, 2021). In response to warmer temperatures and lower water availability, crop areas are shifting to higher latitudes and altitudes, advancing approximately 160 km northwards and 180 m in altitude for every 1 °C increase in annual temperature (Muluneh, 2021; Ouyang *et al.*, 2017). Meanwhile, urban expansion into agricultural areas seriously compromises food productivity in the remaining arable lands (D'Amour *et al.*, 2017). In this context, the intensification of urban agriculture, relying on the use of greenhouses or growth chambers, could be a solution to enhance productivity and mitigate the effects of climate change (Agbonlahor *et al.*, 2007; Taylor, 2020). However, this requires optimising the environmental conditions to maximise the crop's carbon assimilation and yield.

In confined cultivation systems, light and temperature play a central role as the main regulatory factors of gas exchange, growth, biomass accumulation and partition towards the different organs. Although light intensity is reduced in these systems compared to outdoor cultivation conditions, light spectrum, duration and light/dark cycles can be precisely modulated, enabling the optimisation of physiological processes based on the crop and production objective (Modarelli *et al.*, 2022; Paradiso & Proietti, 2022). Therefore, studying the impact of light environment on plant functioning under artificial growth conditions deserves special attention.

Modification of the length of light and dark periods regulates carbon fixation and storage (light period), while also influencing carbon respiration and reserve depletion (night period). Long photoperiods, although useful to promote carbon gain, can induce photoinhibition and feedback mechanisms in plants, reducing the photosynthetic efficiency (Velez-Ramirez *et al.*, 2011). This photoinhibition occurs to avoid damage to photosystems when prolonged exposure to light generates an excess of light energy that cannot be used by the photosynthetic apparatus (Takahashi & Badger, 2011). On the other hand, short photoperiods favour vegetative growth and biomass accumulation in annual plants by increasing chlorophyll content and photosynthetic rate. Notably, Zhang *et al.* (2019) reported an increase in photosynthetic productivity in algae under short and frequent light periods (3:3 seconds and 5:5 seconds), compared to standard photoperiods (12 h light/12 h dark). However, in *Arabidopsis thaliana*, conventional 12 h light/12 h dark cycles that align with the plant's circadian rhythm have been shown to enhance photosynthetic activity, stomatal conductance and growth, compared with both shorter (10 h light/10 h dark) and longer (14 h light/14 h dark) cycles (Dodd *et al.*, 2005). Yet, under their natural environment, plants display a circadian clock that regulates various molecular and physiological processes underlying growth, stomatal opening and photosynthesis. This circadian rhythm

is an endogenous, self-sustaining oscillations that have a period of about 24 h (Taiz *et al.*, 2015). It is influenced by external cues such as light and temperature, as well as by internal cues such as sugar levels in leaves (Jackson, 2009; Westgeest *et al.*, 2023). For example, stomata typically open in the morning in response to light and close at night, a pattern influenced by circadian clock control over the activity of a proton pump in guard cells (Osnato *et al.*, 2022; Westgeest *et al.*, 2023). The expression of photosynthesis-related genes is synchronised with daily variation in light intensity. Specific proteins regulate the activation of these genes, ensuring that photosynthetic reactions reach their maximum efficiency during the day and are reduced at night to conserve energy (Venkat & Muneer, 2022). Moreover, the rate of starch degradation during the night appears to be adjusted to ensure a continuous carbon supply, thus avoiding carbon starvation during prolonged periods of darkness (Feugier & Satake, 2013).

In non-climacteric fruit crops such as grapevine, ripening berries act as strong sugar sinks, triggering the cessation of vegetative growth cessation and reprogramming of metabolic pathways (Savoi *et al.*, 2021). Thus, when analysing the effects of contrasted light/dark cycles on carbon allocation and growth, it is important to distinguish between the pre- and post-ripening phases. Moreover, studying the impact of light/dark cycles in perennial fleshy-fruit crops in controlled growth chamber environments presents numerous technical challenges. The long reproductive development cycle requires exposure to precise and controlled environmental conditions over long periods, which is difficult and costly. The large size of perennial fleshy-fruit species is a supplemental constraint for working under small experimental structures. Moreover, the predisposition of these species to fungal pathogens represents a limiting factor, since the conditions of confinement in the chambers are usually associated with high levels of relative humidity. The microvine (*Vitis vinifera* L.) is a naturally occurring heterozygous mutant of a gene that regulates hormonal signalling (gibberellins) in grapevines (Boss & Thomas, 2002). This mutant presents interesting characteristics to face the above limits, such as miniaturisation (cultivation at 15-25 plants m<sup>-3</sup>), short juvenile period (3-4 months), continuous and indeterminate fruiting (Pellegrino *et al.*, 2019) and tolerance to downy mildew and powdery mildew (Feechan *et al.*, 2013). In addition, the microvine has been validated as a model of grapevine to study the effects of environmental factors on physiological and reproductive processes (Luchaire *et al.*, 2017; Sánchez-Gómez *et al.*, 2018), as well as for genetic and genomic research (Chaïb *et al.*, 2010; Iocco-Corena *et al.*, 2021; Torregrosa *et al.*, 2019).

Finally, the present study aimed to improve our understanding of grapevine physiology under contrasting light/dark cycles, with the objective of optimising production in artificial growing systems that may gain importance in the context of climate change, rather than replicating field viticulture conditions. We focused specifically on the pre-ripening phase, during which vegetative growth remains active.

A 12 h light/12 h dark cycle was applied as a control to represent circadian alignment. We then investigated whether imposing shorter, repeated light/dark cycles (3 h/3 h, repeated four times over 24 h) could desynchronise key physiological processes, potentially enhancing carbon gain and plant growth.

## MATERIALS AND METHODS

### 1. Plant material and periods of light treatments

This study was performed with two genotypes of microvine, number 16 (GENOT 16) and 102 (GENOT 102), resulting from the cross between the *Vitis vinifera* female microvine V3 (Chaïb *et al.*, 2010) and the interspecific hybrid G5 (Ojeda *et al.*, 2017). These sibling lines were selected due to their phenotypic differences, particularly in leaf size and growth rate, to evaluate genotype × environment interactions. The plants were two years old and had been propagated from cuttings and grown in 3 L pots filled with standard loam mix (Alcântara-Novelli Dias *et al.*, 2019). Prior to being exposed to fully controlled climatic conditions, plants were grown in a greenhouse (25 °C/15 °C) until they reached approximately 48 unfolded leaves. As described in Torregrosa *et al.* (2019), plants were trained to maintain a single proleptic axis, removing axillary sylleptic shoots as soon as they appeared.

At the beginning of the experimental period ('T0'), all plants were phenotyped to select a set of plants showing the same number of leaves and inflorescences and similar developmental sequences. All leaves and inflorescences below the thirtieth phytomer from the apex were then removed, leaving each plant with 30 leaves and approximately 15 inflorescences at time T0.

The oldest inflorescence at T0 was in the flowering stage (50 % flowering) and was designated as 'ClusterFlow-T0'. The onset of berry ripening in the grapevine, marked by fruit softening, is associated with the beginning of sugar loading ('BLSugar'). The onset of sugar accumulation was determined by assessing berry softening through gentle compression of the berries on pre-labelled ClusterFlow-T0 bunches. Sugar loading was considered to have begun when softening was detected in the first berry of the ClusterFlow-T0 cluster. Sugar and water are concomitantly

imported in berries from this stage until phloem loading stops (Shahood *et al.*, 2020). This latter stage, which corresponds to the maximum content in water and carbon solutes per berry ('StopLSugar') and maximum berry volume (Bigard *et al.*, 2019), was chosen as the final point of the experiment ('Tfinal'). The end of the sugar loading phase was defined as the point at which the average berry volume of the ClusterFlow-T0 group reached its maximum. This method was used and described by Daviet *et al.* (2023). One plant per genotype and treatment was selected for monitoring by imagery of berry growth on ClusterFlow-T0 to determine the StopLSugar stage.

Based on the changes in ClusterFlow-T0 development, two periods were separated during the trial in the growth chamber. The Period 1 (P1) spanned from flowering to BLSugar stage of ClusterFlow-T0, and the Period 2 (P2) from BLSugar to the StopLSugar stage of ClusterFlow-T0 (Figure 1).

The phyllochron was calculated as the ratio between the accumulated number of phytomers (Acc.Phytomers) and the accumulated degree-days (Acc.GDD, Equation 1) for each plant. A running average phyllochron over three consecutive measurement times ( $t = i$  to  $t = i + 2$ ) was calculated (Equation 2).

$$Acc.GDD_{t=i \text{ to } t=i+2} (^{\circ}Cd) = \int_{t=i \text{ to } t=i+2} \left( \frac{T_{maxd} + T_{mind}}{2} - T_b \right) dt \quad (1)$$

where Tmaxd and Tmind are daily maximum and minimum temperature, respectively; Tb is the base temperature (°C) set to 10 °C (Lebon *et al.*, 2004).

$$Phyllochron_{t=i \text{ to } t=i+2} (^{o}Phytomer/^{\circ}Cd) = \frac{Acc.GDD_{t=i \text{ to } t=i+2}}{Acc.Phytomers_{t=i \text{ to } t=i+2}} \quad (2)$$

While the phyllochron was stable over P1, it gradually increased during P2. Thus, the average phyllochron (at P1) and the rate of phyllochron increase (at P2) were both determined. Because of this instability of phyllochron during P2, all measurements presented in this study were carried out during P1, specifically in period AB, which was common to both genotypes (Figure 1). Only the results of dry mass produced per plant (DMtotal) were obtained at the end of P2 (at Tfinal).

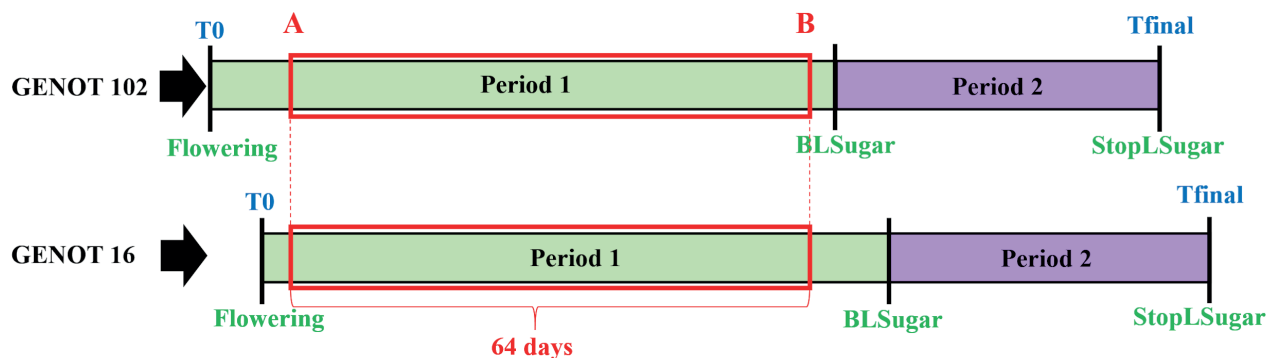


**FIGURE 1.** The two periods of the cycle (from T0 to Tfinal) are based on berry development for each genotype. AB represents the common 64-day period delimited during P1 for the two genotypes.

## 2. Experimental conditions

From T<sub>0</sub> to T<sub>final</sub>, two cycles of photoperiod, T12/12 and T3/3, were compared (Figure S1) while maintaining similar per 24 h amounts of GDD, PAR and VPD. T12/12 treatment corresponded to a standard light/dark cycle with 12 h/12 h day/night, while for the PHOTO 3/3, the light/dark cycle was shortened to 3 h/day and 3 h/night repeated four times over 24 h. For both treatments, day (d) and night (n) climatic conditions were set as follow: temperature of 28 °C/15 °C (d/n), Vapour Pressure Deficit (VPD) of 1 KPa/0.5 Kpa (d/n) and Photosynthetically Active Radiation (PAR) provided by sodium and mercury lamps of 500  $\mu\text{mol s}^{-1} \text{m}^{-2}$ /0  $\mu\text{mol s}^{-1} \text{m}^{-2}$  (d/n). In both treatments, the accumulated PAR over 24 h reached ca. 22  $\text{mol m}^{-2} \text{day}^{-1}$ .

Watering was provided on demand three times a week, to maintain the substrate close to its full water capacity (400 to 500  $\text{mL plant}^{-1} \text{day}^{-1}$ ). Fertilisation was performed once a week, providing 100 mL of liquid plant FD11 diluted to 10 % for each plant. Pest control was implemented through biological control, with inoculations of aphid and scale predator larvae or eggs every 15 days.

## 3. Dry mass produced per plant

At T<sub>final</sub>, vegetative and reproductive organs were sampled separately. Vegetative organs (leaves, petioles and internodes) at each rank position were oven-dried at 60 °C for seven days before being weighed. The fresh weight and number of berries of each cluster were recorded. Berries and cluster stems were stored at -40 °C. The clusters were then crushed separately from the stems using a Qiagen TissueLyser II sample disruptor for green berries and liquid nitrogen in a mortar grinder (Pulverisette 2, Lavallab) for ripening berries. An aliquot of the powder obtained was lyophilised for 72 h using a freeze-dryer (Alpha 2-4, Martin Christ, Osterode, Germany) and weighed to calculate the bulk dry mass. Then, the total dry mass of annual organs (DM<sub>total</sub>) was estimated at T<sub>final</sub>.

To evaluate the efficiency of resources used by the plants, the Water and Radiation Use Efficiency (WRUE) was calculated at T<sub>final</sub>, considering the total annual biomass produced per total amount of water supplied and cumulated incident light from T<sub>0</sub> to T<sub>final</sub>. The WRUE was calculated per plant using (Equation 3):

$$WRUE (\text{mg L}^{-1}/\text{mol m}^{-2}) = \frac{\text{Total DM (mg)}}{(\text{Acc. Water (L)} \times \text{Acc. PAR (mol m}^{-2}))} \quad (3)$$

where: Total DM (mg) is the total annual biomass produced per plant at T<sub>final</sub>; Acc.Water (L) is the accumulated amount of water supplied to fit the demand at T<sub>final</sub>; Acc.PAR (mol m<sup>-2</sup>) is the accumulated amount of incident light at T<sub>final</sub>.

## 4. Temporal leaf growth inferred from its spatial position along the axis

Individual leaf growth along the main axes was measured at the end of period AB (part of P1). For this purpose, only new leaves that grew during this period were considered.

We used an allometric relationship parameterised by Luchaire *et al.* (2017) to estimate the individual leaf area (LA) from the length of the main vein of the leaves (LL) (Equation 4):

$$LA (\text{cm}^2) = 0.0096 LL^2 (\text{mm}^2) + 0.1343 LL (\text{mm}) \quad (4)$$

The total plant leaf area (LA<sub>AB</sub>) was obtained by summing up the individual and adult LA of all leaves per plant produced during period AB.

In addition, the temporal dynamics of leaf growth were inferred from the spatial changes of LA along the axis measured at the end of period AB. The phytomer rank position from the apex (*i.e.*, the Plastochron Index, PI) was converted into thermal time (Acc.GDD), as described by Luchaire *et al.* (2017). Yet Acc.GDD at each PI was calculated from the product of PI<sub>*i*</sub> number and the average phyllochron of PI (period 1) (Equation 5).

$$\text{Acc.GDD}_{PI=i} = PI_i \times \text{Phyllochron} \quad (5)$$

Lastly, one disk sample of 30 mm<sup>2</sup> in diameter was taken on young mature leaves at PI = 10 at the middle and end of period AB. The samples were oven-dried at 60 °C for 24 h and weighed to calculate the Specific Leaf Area (SLA, mm<sup>2</sup> mg<sup>-1</sup>), *i.e.*, the ratio between the area of the disk and its dry mass weight.

## 5. Leaf carbon gain and water loss

Leaf net photosynthesis (An), dark respiration (Rd) and fluorescence measurements were performed on PI = 10 (daytime measurements) and on PI = 11 (night-time measurements) for three plants per genotype and treatment during period AB. All measurements were performed with an infra-red gas analyser (LI-6800; LI-COR Biosciences, Lincoln, NE, USA) equipped with a chamber enclosing 6 cm<sup>2</sup> of leaf area and a multiflash fluorometer. The enclosed leaf was acclimated to the chamber conditions for 5 min before measurements.

Leaf chamber conditions were set with an air flow rate of 600  $\mu\text{mol s}^{-1}$  and a CO<sub>2</sub> concentration of 400 ppm. For night-time measurements, photosynthetically active radiation (PAR) was maintained at 0  $\mu\text{mol m}^{-2} \text{s}^{-1}$ , with a VPD of 0.5 kPa and a leaf temperature of 15 °C. For daytime measurements, PAR was set to 500  $\mu\text{mol m}^{-2} \text{s}^{-1}$ , VPD to 1 kPa and leaf temperature to 28 °C.

Hourly changes of An and Rd were assessed for each treatment. For T12/12 treatment, Rd was measured at five time points during the night (0.5 h, 1.5 h, 2.5 h, 6 h, and 10 h after lights switched off), and An at five time points during the day (0.5 h, 1.5 h, 2.5 h, 6 h, and 10 h after lights switched on). In the T3/3 treatment, Rd was measured at three time points during the night (0.5 h, 1.5 h, and 2.5 h after lights switched off), and An at three time points during the day (0.5 h, 1.5 h, and 2.5 h after lights switched on).

Photosystem performance was assessed by fluorescence measurements taken just before the end-of-day An and the end-of-night Rd measurements described above. Chlorophyll

fluorescence parameters  $F_o$ ,  $F_m$  and  $R_d$  were measured 10 h after lights were switched off in the T12/12 treatment and 2.5 h after lights were switched off in the T3/3 treatment. Chlorophyll fluorescence parameters  $F_m'$ ,  $F_o'$ ,  $F_s$ , and  $A_n$  were measured 10 h after the lights were switched on in the T12/12 treatment and 2.5 h after the lights were switched on in the T3/3 treatment. The chlorophyll fluorescence data were used to calculate photosynthetic performance parameters: electron transport rate (ETR), photochemical quenching (qP) and non-photochemical quenching (qN), and quantum yield of photosystem II ( $\phi$ PSII), as described by Villalobos-González *et al.* (2022).

The accumulated  $A_n$  and  $R_d$  over a 24-hour period were then calculated from hourly measurements. For this purpose, linear functions were calculated between each pair of measurement points. The area under the curve was computed to obtain the accumulated  $A_n$  ( $\int A_n$ ), while the area above the curve was used to determine the accumulated  $R_d$  ( $\int R_d$ ). For the T3/3 measurements, data were obtained by multiplying the results for the 3-hour accumulations by four to obtain the 24-hour period values for both  $A_n$  and  $R_d$ . During the transitions when the lights were switched on or off, no measurements were taken. However, the values from the first and last measurements of each light and dark period were used to complete the curves and perform the integrals. Additionally, the daily carbon gain (Daily C gain) was calculated as the difference between  $\int A_n$  and  $\int R_d$ .

During the same 24-hour measurement period, transpiration per plant was recorded by measuring the weight difference of the pots. The plants were fully watered and, after drainage, the initial pot weight ( $W_i$ ) was recorded. The surface of the substrate in contact with the air was covered to prevent direct evaporation of water. After 24 h, the final pot weight ( $W_f$ ) was recorded. The daily transpiration per unit of LA (Daily Tr) was calculated from the pot weight variations and the LA per plant ( $m^2 \text{ plant}^{-1}$ ) as described in Equation 6 of this study:

$$\text{Daily Tr (L m}^{-2} \text{ day}^{-1}) = \frac{(W_i \text{ (g)} - W_f \text{ (g)})}{\text{LA}_{\text{tot}} \text{ (m}^2 \text{ plant}^{-1})} \quad (6)$$

where  $W_i$  is the initial weight of the pot,  $W_f$  is the weight of the pot 24 h later, and  $\text{LA}_{\text{tot}}$  is the total LA per plant, considering the leaves grown throughout P1 plus the leaves already existing at T0 (30 leaves per  $\text{plant}^{-1}$ ).

## 6. Carbohydrate and nitrogen contents

The carbohydrate and nitrogen contents of the leaves were analysed using the same leaves selected for the  $A_n$  and  $R_d$  dynamics measurements. The C:N ratio for each measurement time was calculated as the percentage of carbon divided by the percentage of nitrogen. The leaf samples were taken after 10 h of darkness in T12/12 and 2.5 h of darkness in T3/3 (leaf at PI = 11) and after 10 h of light in T12/12 and 2.5 h of light in T3/3 (leaf at PI = 10).

For carbohydrate determination, a sample composed of six leaf disc samples per leaf was taken. All samples were

stored at  $-20^\circ \text{C}$  until lyophilisation using the Alpha 2-4 freeze dryer for 48 h. After lyophilisation, four discs per leaf were ground using the TissueLyser II sample disruptor. Soluble metabolites were extracted in three phases with 80 % ethanol, 30 % ethanol, and MilliQ water, recovering the supernatants. Starch extraction from the same samples was performed using amyloglucosidase in acetic buffers. Both extractions followed the protocol outlined by Garcia and Renard (2014). The samples were analysed using a CLARIOstar® Plus multimode plate reader (BMG LABTECH, Ortenberg, Germany).

To determine the percentage of nitrogen and carbon in the leaves, the two remaining lyophilised disc samples were analysed using the Vario Pyro Cube auto analyser (Elementar, Lyon, France) and mass spectrometer, providing two replicates per leaf.

## 7. Statistical analyses

Similarly to Luchaire *et al.* (2017), the temporal variations in LA were inferred from spatial observations of PI along the main axis at the end of period AB using Equation 7. LA was fitted for each plant using the following nonlinear model (Equation 7

$$\text{LA (cm}^2) = \frac{a \times \text{Acc.GDD}^b}{(c^b + \text{Acc.GDD}^b)} \quad (7)$$

where  $a$  is the maximum LA;  $b$  is the shape of the curve;  $c$  is the Acc.GDD to reach half of the maximum LA.

Three variables were calculated from the regressions obtained. They included the LA at full expansion ( $\text{fexp}$ ), set to 90 % of parameter 'a' ( $a_{90}$ ); and the accumulated growing degree days ( $\text{GDD.fexp}$ ) and the plastochron index ( $\text{PI.fexp}$ ) to reach  $a_{90}$ .

To obtain the regression curves that adjusted the evolution of LA based on the Acc.GDD, the statistical software SigmaPlot (*SigmaPlot V16 – Graffiti LLC*, n.d.) was used. To compare the regressions across different treatments and genotypes, the Snedecor's F test and *post hoc* tests were employed with Jamovi (*Jamovi – Open Statistical Software for the Desktop and Cloud*, n.d.). Ultimately, principal component analysis (PCA) was conducted using the *prcomp()* function in RStudio (*RStudio Is Now Posit! – Posit*, n.d.). Additionally, the correlation matrix among the variables was computed to evaluate their relationships by the *cor()* function in R.

The methodology employed relied on a completely randomised experimental design with a factorial arrangement, accounting for two factors: light/dark cycle (T3/3 and T12/12) and genotype (GENOT 16 and GENOT 102).

The comparison of mean variable values between treatments and genotypes was performed using ANOVA, followed by *post hoc* tests at a significance level of  $p = 0.05$ , using the statistical software Jamovi.

## RESULTS

### 1. Leaf development rate and berry phenology

Two experimental periods (P1, P2) were distinguished based on berry development (Figure 1) and phyllochron values. During P1, the phyllochron was rather stable, reaching ca. 23 °Cd phytomer<sup>-1</sup>, regardless of the treatments and genotypes (Table 1). When the oldest bunch of the plant started ripening (beginning P2), the phyllochron increased at the rate of 1 phyllochron day<sup>-1</sup> in all treatments and genotypes.

The total cycle duration of the trial from T0 to Tfinal (Cycle length) varied between treatments, with 98 days for T3/3 and 91 days for T12/12. This difference was mainly due to the extension of P1 (seven days) under T3/3, as the duration of P2 was similar among the two treatments. The two genotypes (GENOT 16 and GENOT 102) displayed similar durations of P1, P2 and cycle.

### 2. Dry mass production and partitioning

The total dry mass of annual organs (DMtotal) measured at Tfinal was similar between the two treatments (T3/3 and T12/12) for each genotype. However, DMtotal was about 23 g higher for GENOT 102 compared to GENOT 16 (Table 2).

Ultimately, regarding biomass partitioning, GENOT 102 allocated more biomass into reproductive organs (bunches, +9 %) and less to vegetative organs (leaves, internodes, and petioles, -9 %) compared to GENOT 16, regardless of the treatment (Table 2).

Daily Tr at the end of P1 reached 0.6 L m<sup>-2</sup> day<sup>-1</sup>, regardless of the treatments and genotypes. In addition, the accumulated water intake and the incident PAR required to produce plant

biomass from T0 to Tfinal (periods 1 and 2) were determined through the variable WRUE. In spite of the longer Cycle length for T3/3 compared to T12/12, WRUE did not differ, reaching 1.8 mg L<sup>-1</sup>/mol m<sup>-2</sup> for both treatments and genotypes.

### 3. Leaf growth dynamics

The temporal leaf growth (LA<sub>AB</sub>) inferred from the spatial patterns along the axis at the end of period AB was analysed in Figure 2. Leaf growth curves were similar among treatments for GENOT 102. In contrast, the growth curves of GENOT 16 were not only lower than those of GENOT 102, but also lower under T12/12 compared to T3/3.

Thus, the fully expanded leaf area (a90) varied between 79 cm<sup>2</sup> for GENOT 16 to 110 cm<sup>2</sup> for GENOT 102 (Table 3). No differences in a90 were found between treatments when considering the two genotypes together. However, the initial leaf expansion rate (parameter b) was 52 % higher for T3/3 than T12/12.

Full leaf expansion was reached, on average, in all plants 252 °Cd after the appearance of the phytomer (GDD.fexp), which corresponds to PI = 10 (PI.fexp), regardless of genotype and treatments.

The leaf thickness analysed from the SLA (mm<sup>2</sup> mg DM<sup>-1</sup>) at PI = 10 was similar for both treatments (Table 3). However, it differed between genotypes. SLA was 13.43 % higher (thinner leaves) for GENOT 102 compared to GENOT 16.

Lastly, the total plant LA produced over the period AB (LA<sub>AB</sub>) was higher (+23.35 %) in GENOT 102 compared to GENOT 16, and it was also higher (+23.10 %) for both genotypes under T3/3 treatment relative to T12/12.

**TABLE 1.** Effect of treatments and genotypes on phyllochron (average value for P1 or slope of variation as a function of time for P2), length of P1 and P2 periods and total cycle duration.

	Period 1				Period 2				Cycle length (Days)	
	Phyll 1 (°Cd phytomer <sup>-1</sup> )		LP 1 (Days)		Slope Phyll 2 (phyllochron day <sup>-1</sup> )		LP 2 (Days)		Mean	SE
Treatment	Mean	SE	Mean	SE	Mean	SE	Mean	SE	Mean	SE
T12/12	23.6 ±	0.594	63.4 ±	1.25	0.655 ±	0.412	28.1 ±	1.2	91.6 ±	0.202
T3/3	22.4 ±	0.519	70.7 ±	2.17	1.3 ±	0.235	27.8 ±	2.3	98.5 ±	0.224
<i>p</i> -value	ns		**		ns		ns		*	
Genotype	Mean	SE	Mean	SE	Mean	SE	Mean	SE	Mean	SE
GENOT 16	22.6 ±	0.716	67.8 ±	2.7	1.26 ±	0.39	26.7 ±	1.43	94.5 ±	1.57
GENOT 102	23.4 ±	0.469	65.9 ±	1.86	0.689 ±	0.327	29.1 ±	1.82	95 ±	1.41
<i>p</i> -value	ns		ns		ns		ns		ns	
Treatment × Genotype	Mean	SE	Mean	SE	Mean	SE	Mean	SE	Mean	SE
<i>p</i> -value	ns		ns		ns		ns		ns	

\* indicates a significance level of *p*-value < 0.05, and ns denotes a result that is not statistically significant, \*\* indicates a significance level of *p*-value < 0.01.

**TABLE 2.** Effect of treatment and genotype on daily transpiration per leaf area (Daily Tr) and Water and Radiation Use Efficiency (WRUE) at the end of P1, and on percentage of dry mass allocation to vegetative (% Vegetative organs) and reproductive organs (% Reproductive organs) and on total dry mass production (DM total) at the end of P2.

	End of Period 1				End of Period 2				DMtotal (g)	
	Daily Tr ( $L\ m^{-2}\ day^{-1}$ )		WRUE ( $mg\ L^{-1}/mol\ m^{-2}$ )		% Vegetative organs		% Reproductive organs			
Treatment	Mean	SE	Mean	SE	Mean	SE	Mean	SE	Mean	SE
T12/12	0.544	± 0.063	1.84	± 0.248	32.9	± 2.23	67.1	± 2.23	67.4	± 7.84
T3/3	0.598	± 0.017	1.82	± 0.19	29	± 4.14	71	± 4.14	82.9	± 9.16
p-value	ns		ns		ns		ns		ns	
Genotype	Mean	SE	Mean	SE	Mean	SE	Mean	SE	Mean	SE
GENOT 16	0.602	± 0.061	1.53	± 0.114	36.2	± 2.59	63.8	± 2.59	61.9	± 5.83
GENOT 102	0.54	± 0.023	2.09	± 0.223	26.7	± 2.58	73.3	± 2.58	85.4	± 8.54
p-value	ns		ns		*		*		*	
Treatment × Genotype	Mean	SE	Mean	SE	Mean	SE	Mean	SE	Mean	SE
p-value	ns		ns		*		*		ns	

\* indicates a significance level of  $p$ -value < 0.05, and ns denotes a result that is not statistically significant, \*\* indicates a significance level of  $p$ -value < 0.01.

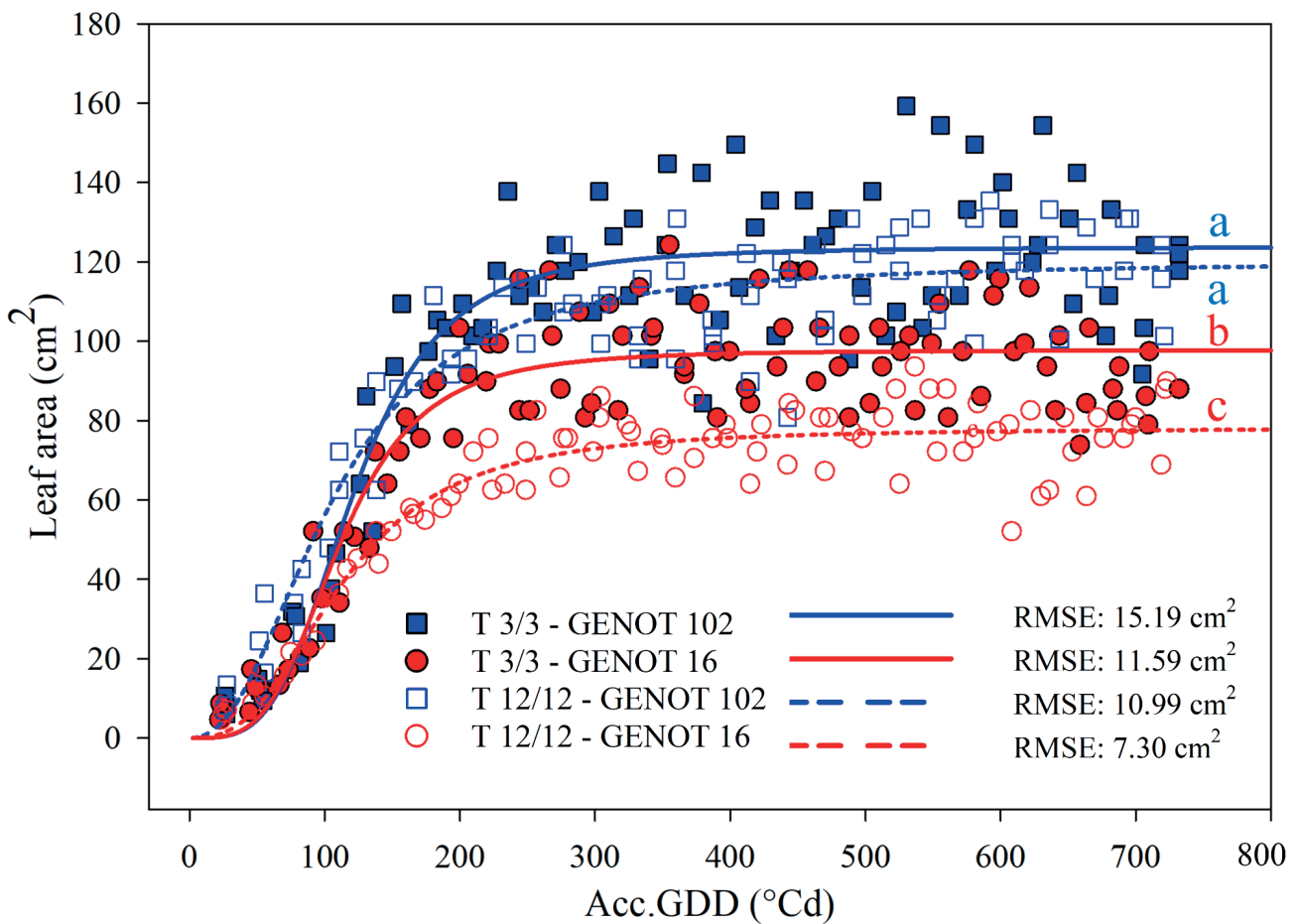


**FIGURE 2.** Temporal dynamics of leaf area during period AB as a function of Acc.GDD was inferred from spatial patterns along the axis at the end of Period AB for each genotype and treatment.

Letters represent the significance of the difference between regressions for each genotype and photoperiod. RMSE stands for root mean square error of the fitting lines.

**TABLE 3.** Variables calculated from the fitting lines of LA<sub>AB</sub> as a function of Acc.GDD (b, a90 and GDD.fexp; Figure 2), Specific Leaf Area (SLA) measured at PI = 10 and sum of individual LA of leaves per plant during phase AB (LA<sub>AB</sub>).

Treatment	parameter b		a90 (cm <sup>2</sup> )		GDD.fexp (°Cd)		PI.fexp		SLA		LA <sub>AB</sub>	
	Mean	SE	Mean	SE	Mean	SE	Mean	SE	Mean	SE	Mean	SE
T12/12	2.58	± 0.334	90.1	± 8.78	294	± 37.7	11.5	± 1.43	20.5	± 0.772	2,242	± 195
T3/3	3.93	± 0.36	99.6	± 6.97	210	± 15.4	8.67	± 0.558	22.3	± 1.06	2,760	± 148
<i>p</i> -value	*		ns		ns		ns		ns		*	
Genotype	Mean	SE	Mean	SE	Mean	SE	Mean	SE	Mean	SE	Mean	SE
GENOT 16	3.37	± 0.434	79.3	± 4.78	236	± 30.4	10	± 1.21	20.1	± 0.538	2,239	± 207
GENOT 102	3.13	± 0.478	110	± 3.89	268	± 36.7	10.2	± 1.3	22.8	± 1.11	2,762	± 128
<i>p</i> -value	ns		**		ns		ns		*		*	
Treatment × Genotype	Mean	SE	Mean	SE	Mean	SE	Mean	SE	Mean	SE	Mean	SE
<i>p</i> -value	ns		ns		ns		ns		ns		ns	

\* indicates a significance level of *p*-value < 0.05, and ns denotes a result that is not statistically significant, \*\* indicates a significance level of *p*-value < 0.01.

#### 4. Leaf carbon gain

Under T3/3, photosynthesis (An) varied slightly during the 3-hour light period for both genotypes (Figure 3). In contrast, under T12/12, a large decrease was observed at 3 h and 1.5 h after the light was turned on for GENOT 102 and 16, respectively.

Thus, although An at the end of the light period was similar for both genotypes, it was 68 % higher for T3/3 compared to T12/12 (Table 4).

Rd was the highest 30 min after darkness for both genotypes and the two treatments (Figure 3). Then it stabilised at a lower rate, which was similar for both genotypes, but lower (–51 %) for T3/3 compared to T12/12 at the end of the night (Table 4).

The efficiency of photosynthesis was also addressed at the end of the day (ED). No difference in any photosystem efficiency parameters was observed between the genotypes (Table 4). However, the higher An rate for T3/3 compared to T12/12 coincided with lower (–20 %) non-photochemical energy losses (qN) and higher (+7.9 %) energy use for assimilate production (qP). T3/3 also displayed higher Electron Transport Rate (ETR, +28 %) and efficiency of Photosystem II (φPSII, +28 %) compared to T12/12.

Finally, accumulated photosynthesis (∫An), accumulated dark respiration (∫Rd) and daily carbon gain (Daily C gain) over 24 h were calculated for each combination of treatment and genotype (Table 5). An increase of 54 % in ∫An and 66 % in Daily C gain was observed under T3/3 compared to T12/12. There were no differences in ∫An between genotypes; however, GENOT 102 showed a Daily C gain 20 % higher than GENOT 16. Additionally, no differences were observed in accumulated respiration (∫Rd) both between genotypes and treatments.

#### 5. Leaf carbon and nitrogen status

Measurements of carbohydrate content in adult leaves (PI = 10) were made at two different times of the day: at the end of the night (EN) and at the end of the day (ED) (Table 6). No differences were found between T3/3 and T12/12 in starch, soluble sugars and total carbohydrate levels at each time point of the cycle. However, GENOT 102 showed higher content of soluble sugars (+28 %) in leaves at EN compared to GENOT 16, while GENOT 16 exhibited higher starch content (+55 %) in leaves at ED compared to GENOT 102, resulting in higher total carbohydrate content (+43 %).

Leaf nitrogen content (% N) was quantified at the same time and for the same leaves as carbohydrate measurements. For both genotypes, higher % N were observed at all measurement points (EN: +15 % and ED: +19 %) under T3/3 compared to T12/12, leading to lower C:N ratio for T3/3 compared to T12/12 (EN: –18 % and ED: –16 %) (Table 6). However, the % N only varied at ED between genotypes, being higher for GENOT 102 (+11 %) compared to GENOT 16, but without impact on the C:N ratio.

#### 6. Multiple variable analysis of carbon and water functioning at the leaf and plant scales

A PCA was conducted to highlight the relationships between the variables measured at leaf or plant levels for each treatment and genotype (Figure 4).

In Figure 4A, the variables measured at leaf level (short term), maximum leaf size (a90), daily carbon gain (Daily C gain), specific leaf area (SLA), total leaf carbon (TC) and leaf C:N ratio (C:N) were considered. These last two variables were measured at two times, at the end of the night (EN) and the end of the day (ED). The first two axes explained 68.38 % of the total variance. On axis 1 (45 %), a90, Daily C gain and SLA were negatively related to C:N (EN and ED). Axis 2 (23 %) was represented by TC (EN, ED).

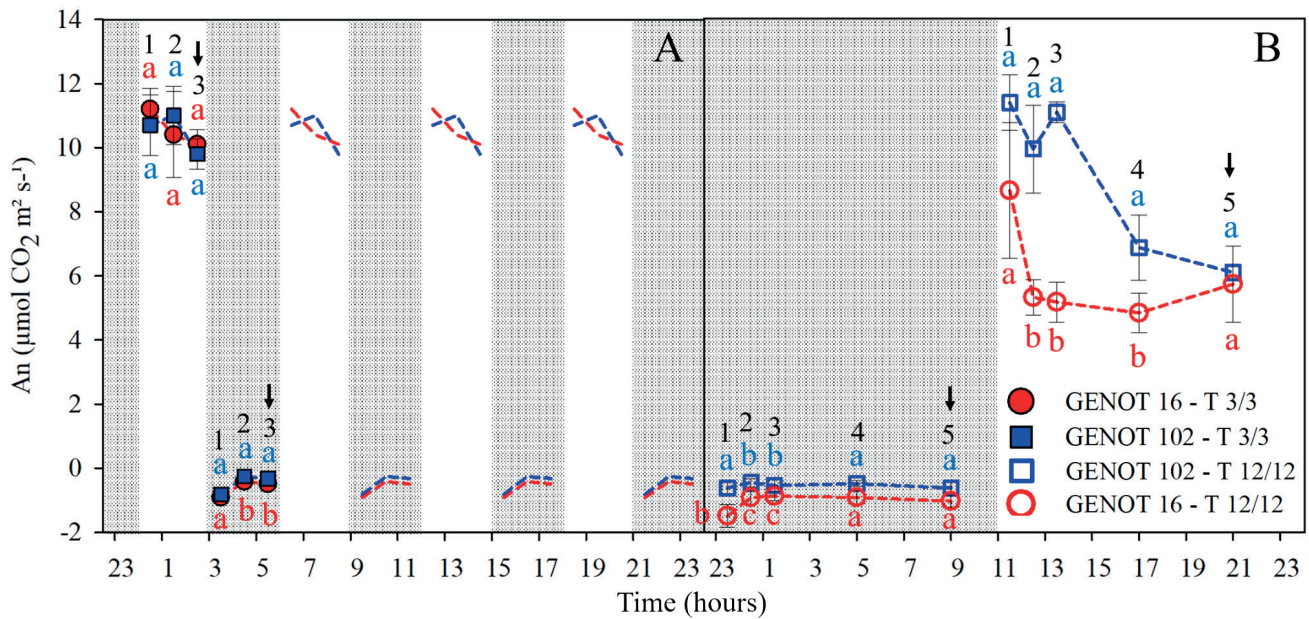


**FIGURE 3.** Dynamics of An and Rd of both genotypes under T3/3 treatment (A) and T12/12 treatment (B). The points numbered from 1 to 5 represent the measurement points over time. The letters indicate significant differences between treatments and genotypes at each measurement point (comparisons within the same measurement point). The arrows indicate the measurement points at the end of the day and the end of the night, whose comparative analysis results are detailed in Table 4.

**TABLE 4.** Effect of treatments and genotypes on Rd measured at the end of the night, and on An and photosynthetic efficiency (non-photochemical quenching (qN), photochemical quenching (qP), electron transport rate (ETR), and the efficiency of Photosystem II ( $\phi$ PSII)), all measured at the end of the day.

	An		Rd		qN		qP		ETR		$\phi$ PSII	
Treatment	Mean	SE	Mean	SE	Mean	SE	Mean	SE	Mean	SE	Mean	SE
T12/12	5.92	± 0.547	-0.827	± 0.146	0.751	± 0.024	0.73	± 0.015	84.9	± 4.67	0.403	± 0.022
T3/3	9.94	± 0.304	-0.409	± 0.048	0.601	± 0.018	0.788	± 0.014	109	± 3.1	0.516	± 0.015
p-value	**		*		**		*		**		**	
Genotype	Mean	SE	Mean	SE	Mean	SE	Mean	SE	Mean	SE	Mean	SE
GENOT 16	7.91	± 1.12	-0.762	± 0.148	0.666	± 0.038	0.776	± 0.015	101	± 5.85	0.479	± 0.028
GENOT 102	7.95	± 0.862	-0.474	± 0.105	0.685	± 0.041	0.742	± 0.02	92.8	± 6.89	0.441	± 0.033
p-value	ns		ns		ns		ns		ns		ns	
Treatment x Genotype	Mean	SE	Mean	SE	Mean	SE	Mean	SE	Mean	SE	Mean	SE
p-value	ns		ns		ns		ns		ns		ns	

\* indicates a significance level of  $p$ -value < 0.05, and ns denotes a result that is not statistically significant, \*\* indicates a significance level of  $p$ -value < 0.01.

The four combinations of treatment and genotype were mainly distributed across axis 1. Both genotypes under T3/3 were positioned to the left of the graph compared to the T12/12 treatment, indicating higher  $a_{90}$ , Daily C gain and SLA and lower C:N ratio for T3/3.

In Figure 4B, the plant-level variables (long term) were considered: total biomass produced per plant (DMtotal), total cycle length (Cycle length), growth rate in P1 (Phyll 1), variation in growth rate in P2 (Slope Phyll 2), leaf area per

plant (LA), efficiency in the use of light and water to produce biomass (WRUE) and dry mass partition (% Vegetative organs and % Reproductive organs).

The principal components PC1 and PC2 explain 69.96 % of the total variability. On axis 1 (52 % of variability), % Vegetative organs is opposite to DMtotal, % Reproductive organs and WRUE. On axis 2 (18 % of variability), Cycle length, Slope Phyll 2 and LA were negatively related to Phyll 1.

**TABLE 5.** Effect of treatment and genotype on accumulated photosynthesis ( $\int An$ ), dark respiration ( $\int R$ ) and daily carbon gain (Daily C gain).

Treatment	$\int An$ (mol CO <sub>2</sub> m <sup>2</sup> day <sup>-1</sup> )		$\int R$ (mol CO <sub>2</sub> m <sup>2</sup> day <sup>-1</sup> )		Daily C gain (mol CO <sub>2</sub> m <sup>2</sup> day <sup>-1</sup> )	
	Mean	SE	Mean	SE	Mean	SE
T12/12	0.293	± 0.028	-0.033	± 0.006	0.26	± 0.032
T3/3	0.452	± 0.017	-0.021	± 0.001	0.432	± 0.016
<i>p</i> -value	**		ns		**	
Genotype	Mean	SE	Mean	SE	Mean	SE
GENOT 16	0.347	± 0.051	-0.033	± 0.005	0.314	± 0.055
GENOT 102	0.399	± 0.026	-0.021	± 0.003	0.378	± 0.028
<i>p</i> -value	ns		ns		*	
Treatment × Genotype	Mean	SE	Mean	SE	Mean	SE
<i>p</i> -value	ns		ns		*	

\* indicates a significance level of *p*-value < 0.05, and ns denotes a result that is not statistically significant, \*\* indicates a significance level of *p*-value < 0.01.

**TABLE 6.** Effect of treatment and genotype on carbohydrate (starch, soluble sugars, and total carbohydrates), nitrogen content (% N) and C:N ratio of leaves at the end of the night (EN) and at the end of the day (ED).

Treatment	Starch (mg g <sup>-1</sup> DM)		Soluble sugars (mg g <sup>-1</sup> DM)		Total carbohydrates (mg g <sup>-1</sup> DM)		% N		C:N		
	Mean	SE	Mean	SE	Mean	SE	Mean	SE	Mean	SE	
<b>End of night (EN)</b>											
T12/12	111	± 19.3	47.9	± 3.53	159	± 19	3.47	± 0.122	13.5	± 0.267	
T3/3	126	± 27.8	54.5	± 3.36	181	± 29.6	3.98	± 0.048	11.4	± 0.448	
<i>p</i> -value	ns		ns		ns		*		**		
Genotype	Mean	SE	Mean	SE	Mean	SE	Mean	SE	Mean	SE	
GENOT 16	124	± 29.7	45	± 3.08	169	± 31.7	3.72	± 0.166	12.7	± 0.535	
GENOT 102	113	± 16.7	57.4	± 1.76	171	± 16.8	3.73	± 0.12	12.1	± 0.607	
<i>p</i> -value	ns		*		ns		ns		ns		
Treatment × Genotype	Mean	SE	Mean	SE	Mean	SE	Mean	SE	Mean	SE	
<i>p</i> -value	ns		ns		ns		ns		ns		
<b>End of Day (ED)</b>											
T12/12	160	± 23.8	48.5	± 1.98	209	± 24.9	2.97	± 0.058	14.1	± 0.249	
T3/3	200	± 24.4	47.1	± 2.06	247	± 26.2	3.54	± 0.186	12.2	± 0.741	
<i>p</i> -value	ns		ns		ns		*		*		
Genotype	Mean	SE	Mean	SE	Mean	SE	Mean	SE	Mean	SE	
GENOT 16	219	± 23.3	49.4	± 2.38	269	± 25.4	3.08	± 0.118	13.8	± 0.576	
GENOT 102	141	± 12.7	46.3	± 1.32	188	± 12.4	3.43	± 0.208	12.5	± 0.719	
<i>p</i> -value	*		ns		*		*		ns		
Treatment × Genotype	Mean	SE	Mean	SE	Mean	SE	Mean	SE	Mean	SE	
<i>p</i> -value	ns		ns		ns		*		ns		

\* indicates a significance level of *p*-value < 0.05, and ns denotes a result that is not statistically significant, \*\* indicates a significance level of *p*-value < 0.01.

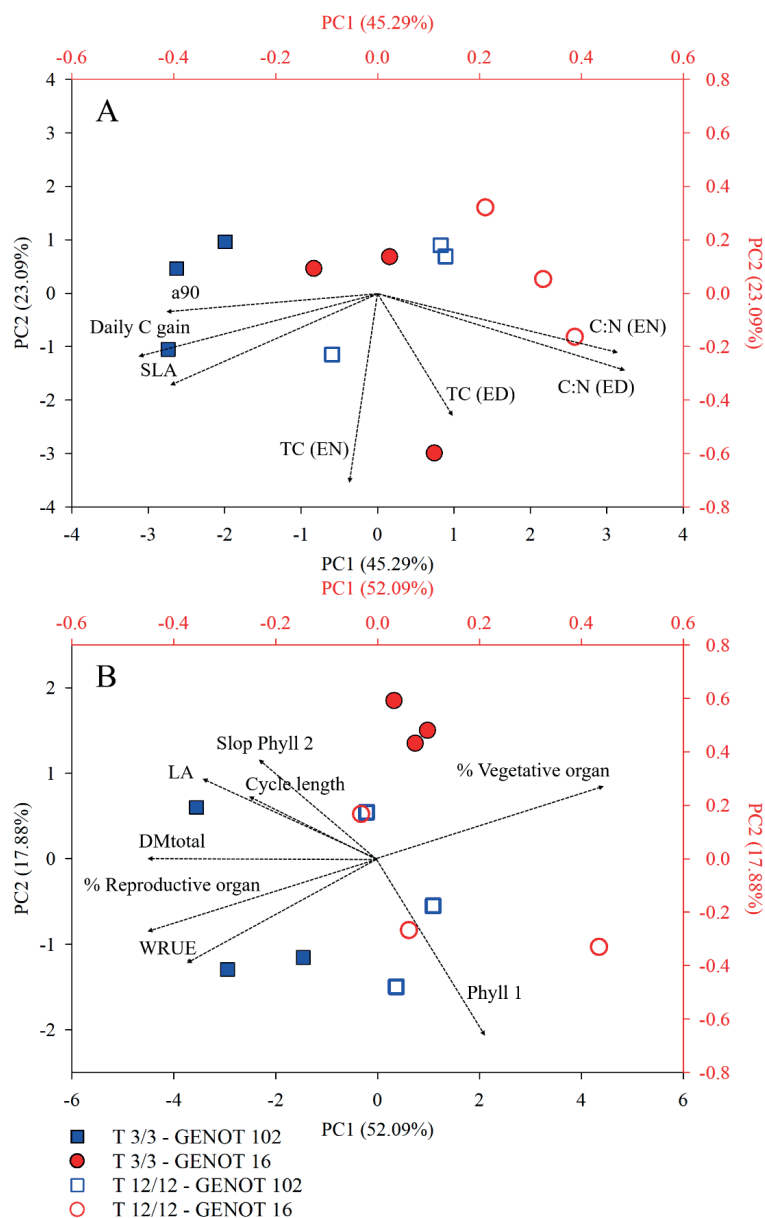


**FIGURE 4.** PCA analysis of variables at leaf level (A) and plant level (B) for each genotype-treatment combination (the first two principal components, PC1 and PC2, are represented). The loading scale is displayed in red and the scores scale in black.

Both genotypes (16 and 102) under T12/12 were grouped in the central part of the graph, indicating an intermediate response in the evaluated variables. However, under T3/3 treatment, GENOT 102 was located towards the left side of axis 1, associated with higher DMtotal, % Reproductive organs and WRUE, while GENOT 16 was positioned at the top of axis 2, standing out for a higher Cycle length, Slope Phyll 2 and LA.

## DISCUSSION

This study presents an innovative experimental design, exploring the effects of two different light/dark regimes with short light/dark cycles (T3/3) compared to a standard light/dark cycle (T12/12) on grapevine functioning. This approach, so far little explored in perennial fleshy fruit crops, allows

one to optimise growth and resource efficiency in a context of intensive production under controlled conditions, laying the foundations for future research in this field.

### 1. Impact of short light/dark cycle on plant and berry development

Microvine leaf development varied over the cropping cycle and could be divided into two distinct phases (P1 and P2). During P1, which covered the period from flowering to the onset of ripening of the oldest cluster (ClusterFlow-T0), plants showed stable values of phyllochron ( $23\text{ }^{\circ}\text{Cd phytomer}^{-1}$ ) and individual leaf growth duration ( $252\text{ }^{\circ}\text{Cd}$  similar for both genotypes and treatments, in agreement with values reported in previous grapevine and microvine studies (Lebon *et al.*, 2004; Luchaire *et al.*, 2017)).

During P2, corresponding to the period from the onset of ripening to maximum berry volume of ClusterFlow-T0, the phyllochron progressively increased (1 phyllochron day<sup>-1</sup>), indicating a slowdown in vegetative development induced by sugar loading in the berries. These findings are consistent with the preferential redistribution of carbon towards the reproductive organs during ripening, which acts as the main carbon sink (Fasoli *et al.*, 2018; Hernández-Montes *et al.*, 2022). This increased carbon demand can create pressure on the plant's carbon balance, especially if carbohydrate supply does not meet this demand, generating carbon starvation and flower abortion (Luchaire *et al.*, 2023). Ultimately, the altered carbon balance as berries start ripening is a point of caution to consider when evaluating any treatment effects on carbon metabolism and resource allocation. Fine control of the leaf:fruit ratio during this period could help reduce carbon strain.

The total duration of berry development (from flowering to maximum berry volume, P1 + P2) ranged from 91 to 98 days, with a duration of the berry ripening period (P2) of approximately 30 days, similar to the phenological times reported in Rienth *et al.* (2016) and Torregrosa *et al.* (2019) where P1 + P2 had a duration of 83 to 100 days and P2 of 37 to 45 days. The short light/dark cycle (T3/3) led to a seven-day delay of P1 compared to T12/12, but did not impact P2 duration. Dormancy-related causes for this delay have been ruled out. Node lignification, a reliable indicator of dormancy in microvines (Alcântara-Novelli Dias *et al.*, 2019), was assessed at T0 and Tfinal, and showed no significant differences between treatments or genotypes, confirming homogeneity with respect to dormancy. The observed delay in the onset of berry ripening under short light/dark cycles could be attributed to the desynchronisation between photosynthetic and metabolic processes regulated by the circadian clock. Under normal conditions (12 h/12 h), the circadian clock adjusts the rate of starch degradation during the night to maintain a continuous carbon supply and avoid periods of scarcity (Feugier & Satake, 2013; Smith & Stitt, 2007). However, accelerated rhythms can alter this synchronisation, reducing the availability of soluble sugars at critical times for transport to developing berries.

Furthermore, since sucrose levels not only serve as an energy source, they also modulate the rhythm of the circadian clock (Venkat & Muneer, 2022). Fluctuating levels in short cycles could interfere with the metabolic signalling necessary to initiate berry ripening and transform them into the most important carbon sink during this stage (Savoi *et al.*, 2021).

On the other hand, the similar duration of the ripening period (P2) for both treatments is consistent with the observations of Davies *et al.* (2023). These authors reported a reduction of the oscillations of the circadian rhythm after the beginning of berry ripening, thus reducing their control over the physiological processes of the vine.

## 2. Impact of short light/dark cycle on growth and carbon distribution

T3/3 favoured the potential carbon production over the cycle compared to T12/12 by increasing the photosynthetic rate and efficiency and lowering the respiration rate. Indeed, under T3/3, both genotypes maintained elevated photosynthetic rates throughout the light cycle, whereas under T12/12, photosynthetic rates were reduced by more than half after approximately 3 h of light exposure. This suggests that short and frequent light periods can maximise photosynthesis and minimise the risk of light-induced oxidative stress (Takahashi & Badger, 2011). In addition, rapid alternation between light and dark periods may favour the recovery of the photosynthetic apparatus, thereby limiting photoinhibition (Venkat & Muneer, 2022; Westgeest *et al.*, 2023), given that dark respiration acts as a fine-tuning mechanism to restore CO<sub>2</sub> levels in mesophyll cells, optimising photosynthesis under short light cycles (Feugier & Satake, 2013). The improvement in photosynthetic efficiency parameters, such as the increase in electron transport rate (ETR) and photosystem II efficiency ( $\phi$ PSII) under T3/3, confirms that the temporal pattern of light and dark exposure can affect photosynthetic efficiency. While our results cannot confirm whether these changes were due to circadian desynchronisation or synchronisation, they do demonstrate that shorter light/night cycles confer an advantage for carbon fixation compared to the standard 12 h/12 h cycle in the microvine. Interestingly, these outcomes contrast with those reported by Dodd *et al.* (2005) in *Arabidopsis thaliana*. Further investigations are needed to clarify whether these responses are linked to endogenous rhythmic regulation or represent a broader adaptive plasticity to changes in the light environment.

This increase in photosynthetic efficiency may be linked to the observed increase in leaf nitrogen in both genotypes under T3/3. Previous research indicates that as leaf nitrogen content increases, the activity of key enzymes in the Calvin cycle, such as Rubisco (ribulose-1,5-bisphosphate carboxylase/oxygenase) also increases and is associated with higher levels of chlorophyll (Pérez Asseff *et al.*, 2023), which is essential for optimal CO<sub>2</sub> assimilation (Reich *et al.*, 1998).

Furthermore, in both genotypes under T3/3, respiration (at the end of the night) decreased by half compared to T12/12. Ultimately, the daily carbon gain was twice as high in T3/3 as in T12/12, and it was also higher for GENOT 102 compared to GENO 16, although to a lesser extent (20 % variation). In contrast, leaf carbon content under T3/3 did not show significant differences compared to T12/12. This suggests that while the short light/dark cycle increases daily carbon gain, it also promotes a higher carbohydrate mobilisation towards sink organs. Plants adjust the distribution of photoassimilates to ensure their constant supply of sugars during the night (Smith & Stitt, 2007; Zeeman *et al.*, 2007). Indeed, a marked increase in individual LA was observed under T3/3 compared to T12/12 for GENOT 16. Increased growth can also induce a temporary reduction of leaf carbon (Chen & Cheng, 2003). The higher individual LA for

GENOT 102 compared to GENOT 16 may be, at least partly, responsible for its lower leaf total carbohydrates (ED).

It was observed that the T3/3 treatment leads to a greater carbon gain, resulting from a higher accumulated daily net photosynthesis and an increase in leaf surface area ( $LA_{AB}$ ), in addition to a longer P1 period. However, the total dry mass (DM<sub>total</sub>) values did not show significant differences between the treatments.

According to the model proposed by Monteith *et al.* (1977) and Monteith *et al.* (1994), the total DM of a plant is determined by the light interception efficiency (related to LA), the light to carbon conversion efficiency (related to An) and the duration of light interception (related to the cycle length). In this context, plants under T3/3 would be expected to present a higher total DM compared to T12/12. Despite observing a trend towards higher total DM values in both genotypes under T3/3, the differences were not statistically significant, possibly due to the small number of samples (29.63 % CV).

In contrast, as expected, the higher carbon gain (+20 %) for GENOT 102 compared to GENOT 16 was consistent with a higher DM<sub>total</sub> (+37 %) (Table 2). Also, GENOT 102 under T3/3 led to a higher biomass allocation towards reproductive organs at the expense of vegetative organs (Figure 4B). In contrast, GENOT 16 did not display any changes in carbon allocation between treatments. In conclusion, GENOT 102 was shown to respond differently than GENOT 16 to short light/dark cycles. The different adaptive strategies to short light/dark cycles between species and genotypes, as reported by Osnato *et al.* (2022), should be further explored.

### 3. Implications for urban agriculture

Both genotypes and treatments showed similar water consumption per m<sup>2</sup> of leaf area per day and comparable WRUE. However, the T3/3 treatment required an additional week due to the extension of P1 to complete the cycle compared to T12/12 (cycle increased by about 6 %). This implies a higher cumulative consumption of resources such as light and water during the total cycle. If we compare the increase in resource consumption under T3/3 with the gain in yield, GENOT 102 compensates for this expenditure with an increase in yield, but GENOT 16 does not. Therefore, while the T3/3 treatment proved beneficial in improving photosynthetic efficiency and promoting carbon allocation, the trade-offs in extended resource use must be carefully weighed. These results underline the importance of adapting genotype selection and photoperiod management as a tool to modulate light/dark cycles to the specific objectives and constraints of agricultural systems, ensuring an optimal balance between productivity and resource efficiency.

Our study provides a novel contribution by demonstrating that the use of short light/dark cycles are effective in perennial crops, such as the microvine, whose development and carbon metabolism are strongly influenced by the interplay between vegetative and reproductive growth phases

(Bigard *et al.*, 2019; Savoi *et al.*, 2021). The application of short light/dark cycles in perennial systems under controlled conditions has not been sufficiently explored, and our results suggest that this approach has great potential for sustainable intensification of agriculture in controlled environments (Chaïb *et al.*, 2010; Torregrosa *et al.*, 2019). Lastly, this study aimed to provide a focused analysis on vegetative development and physiological responses, although data on berry growth and composition (*e.g.*, sugar content and acidity) were also collected during the experiment. The specific impact of light/dark cycles on berry development will be detailed in a separate article.

## CONCLUSION

In conclusion, this study demonstrates that a short light/dark cycle can improve photosynthetic efficiency and daily carbon gain in microvines, suggesting that this approach has significant potential to improve production in controlled/confined agricultural systems. The differences in biomass distribution between genotypes highlight the importance of selecting the appropriate genetic material to maximise productivity under controlled conditions. This study demonstrates that genotypic variability influenced biomass production more than the treatment itself.

These findings open new lines of research on how modulation of the light/dark cycles can optimise crop yield in modern high-tech agriculture and provide a solid foundation for future research on the interaction between light/dark cycle and metabolism in perennial plants.

## ACKNOWLEDGEMENTS

The authors thank Thibaut Perez from the Isotope Quantification platform AQUi, hosted in IPSiM (Institute of Plant Sciences of Montpellier), for leaf carbon and nitrogen content analysis. They also thank Myriam Dautat and Stephane Berthezene from the Montpellier Plant Phenotyping Platform (M3P) for their help with growth chamber monitoring, and Gaele Rolland for accompanying the biochemical assays.

## REFERENCES

- Agbonlahor, M. U., Momoh, S., & Dipeolu, A. O. (2007). International Journal of Urban Vegetable Crop Production and Production Efficiency. *International Journal of Vegetable Science*, 13(2), 63–72. [https://doi.org/10.1300/J512v13n02\\_06](https://doi.org/10.1300/J512v13n02_06)
- Alcântara-Novelli Dias, F., Torregrosa, L., Luchaire, N., Houel, C., & Pellegrino, A. (2019). The microvine, a model to study the effect of temperature on grapevine latent bud development and fruitfulness. *Oeno One*, 53(3), 373–407. <https://doi.org/10.20870/oeno-one.2019.53.3.2313>
- Bhatt, R., & Hossain, A. (2019). Concept and Consequence of Evapotranspiration for Sustainable Crop Production in the Era of Climate Change. In *Advanced Evapotranspiration Methods and Applications*. IntechOpen. <https://doi.org/10.5772/intechopen.83707>

- Bigard, A., Romieu, C., Sire, Y., Veyret, M., Ojeda, H., & Torregrosa, L. (2019). The kinetics of grape ripening revisited through berry density sorting. *Oeno One*, 53(4), 709–724. <https://doi.org/10.20870/oeno-one.2019.53.4.2224>
- Boss, P. K., & Thomas, M. R. (2002). Association of dwarfism and floral induction with a grape “green revolution” mutation. *Nature*, 416(6883), 847–850. <https://doi.org/10.1038/416847a>
- Chaïb, J., Torregrosa, L., MacKenzie, D., Corena, P., Bouquet, A., & Thomas, M. R. (2010). The grape microvine - A model system for rapid forward and reverse genetics of grapevines. *Plant Journal*, 62(6), 1083–1092. <https://doi.org/10.1111/j.1365-313X.2010.04219.x>
- Chen, L. S., & Cheng, L. (2003). Carbon assimilation and carbohydrate metabolism of “Concord” grape (*Vitis labrusca* L.) Leaves in response to nitrogen supply. *Journal of the American Society for Horticultural Science*, 128(5), 754–760. <https://doi.org/10.21273/jashs.128.5.0754>
- D’Amour, C. B., Reitsma, F., Baiocchi, G., Barthel, S., Güneralp, B., Erb, K. H., Haberl, H., Creutzig, F., & Seto, K. C. (2017). Future urban land expansion and implications for global croplands. *Proceedings of the National Academy of Sciences of the United States of America*, 114(34), 8939–8944. <https://doi.org/10.1073/pnas.1606036114>
- Davies, C., Burbidge, C. A., Böttcher, C., & Dodd, A. N. (2023). Loss of Diel Circadian Clock Gene Cycling Is a Part of Grape Berry Ripening. *Plant and Cell Physiology*, 64(11), 1386–1396. <https://doi.org/10.1093/pcp/pcad099>
- Daviet, B., Fournier, C., Cabrera-Bosquet, L., Simonneau, T., Cafier, M., & Romieu, C. (2023). Ripening dynamics revisited: an automated method to track the development of asynchronous berries on time-lapse images. *BioRxiv*. <https://doi.org/10.1101/2023.07.12.548662>
- Dodd, A. N., Salathia, N., Hall, A., Kévei, E., Tóth, R., Nagy, F., Hibberd, J. M., Millar, A. J., & Webb, A. A. R. (2005). Cell biology: Plant circadian clocks increase photosynthesis, growth, survival, and competitive advantage. *Science*, 309(5734), 630–633. <https://doi.org/10.1126/science.1115581>
- Fasoli, M., Richter, C. L., Zenoni, S., Bertini, E., Vitolo, N., Dal Santo, S., Dokoozlian, N., Pezzotti, M., & Tornielli, G. B. (2018). Timing and order of the molecular events marking the onset of berry ripening in grapevine. *Plant Physiology*, 178(3), 1187–1206. <https://doi.org/10.1104/pp.18.00559>
- Feechan, A., Anderson, C., Torregrosa, L., Jermakow, A., Mestre, P., Wiedemann-Merdinoglu, S., Merdinoglu, D., Walker, A. R., Cadle-Davidson, L., Reisch, B., Aubourg, S., Bentahar, N., Shrestha, B., Bouquet, A., Adam-Blondon, A. F., Thomas, M. R., & Dry, I. B. (2013). Genetic dissection of a TIR-NB-LRR locus from the wild North American grapevine species *Muscadinia rotundifolia* identifies paralogous genes conferring resistance to major fungal and oomycete pathogens in cultivated grapevine. *Plant Journal*, 76(4), 661–674. <https://doi.org/10.1111/tpj.12327>
- Feugier, F. G., & Satake, A. (2013). Dynamical feedback between circadian clock and sucrose availability explains adaptive response of starch metabolism to various photoperiods. *Frontiers in Plant Science*, 3(JAN), 1–11. <https://doi.org/10.3389/fpls.2012.00305>
- Garcia, C., & Renard, C. (2014). Validation des dosages enzymatiques des sucres (glucose, fructose, saccharose) et acides (acide citrique et malique) par un spectrophotomètre avec lecteur de microplaques. *Le Cahier Des Techniques de l’INRA*, 81(1), 1–18.
- Hernández-Montes, E., Escalona, J. M., Tomás, M., Martorell, S., Bota, J., Tortosa, I., & Medrano, H. (2022). Carbon balance in grapevines (*Vitis vinifera* L.): effect of environment, cultivar and phenology on carbon gain, losses and allocation. *Australian Journal of Grape and Wine Research*, 28(4), 534–544. <https://doi.org/10.1111/ajgw.12557>
- Iocco-Corena, P., Chaïb, J., Torregrosa, L., Mackenzie, D., Thomas, M. R., & Smith, H. M. (2021). VviPLATZ1 is a major factor that controls female flower morphology determination in grapevine. *Nature Communications*, 12(1). <https://doi.org/10.1038/s41467-021-27259-8>
- Jackson, S. D. (2009). Plant responses to photoperiod. *New Phytologist*, 181(3), 517–531. <https://doi.org/10.1111/j.1469-8137.2008.02681.x>
- Lebon, E., Pellegrino, A., Tardieu, F., & Lecoeur, J. (2004). Shoot development in grapevine (*Vitis vinifera*) is affected by the modular branching pattern of the stem and intra- and inter-shoot trophic competition. *Annals of Botany*, 93(3), 263–274. <https://doi.org/10.1093/aob/mch038>
- Luchaire, N., Rienth, M., Romieu, C., Nehe, A., Chatbanyong, R., Houel, C., Ageorges, A., Gibon, Y., Turc, O., Muller, B., Torregrosa, L., & Pellegrino, A. (2017). Microvine: A new model to study grapevine growth and developmental patterns and their responses to elevated temperature. *American Journal of Enology and Viticulture*, 68(3), 283–292. <https://doi.org/10.5344/ajev.2017.16066>
- Luchaire, N., Torregrosa, L. J.-M., Gibon, Y., Rienth, M., Romieu, C., Ageorges, A., Turc, O., Muller, B., & Pellegrino, A. (2023). A low carbon balance triggers Microvine inflorescence abscission at high temperatures. *Frontiers in Horticulture*, 2(November), 1–14. <https://doi.org/10.3389/fhort.2023.1267429>
- Malhi, G. S., Kaur, M., & Kaushik, P. (2021). Impact of climate change on agriculture and its mitigation strategies: A review. *Sustainability (Switzerland)*, 13(3), 1–21. <https://doi.org/10.3390/su13031318>
- Masia, S., Trabucco, A., Spano, D., Snyder, R. L., Sušnik, J., & Marras, S. (2021). A modelling platform for climate change impact on local and regional crop water requirements. *Agricultural Water Management*, 255(June 2020). <https://doi.org/10.1016/j.agwat.2021.107005>
- Modarelli, G. C., Paradiso, R., Arena, C., De Pascale, S., & Van Labeke, M. C. (2022). High Light Intensity from Blue-Red LEDs Enhance Photosynthetic Performance, Plant Growth, and Optical Properties of Red Lettuce in Controlled Environment. *Horticulturae*, 8(2). <https://doi.org/10.3390/horticulturae8020114>
- Monteith, J. (1977). Climate and the efficiency of crop production in Britain. *Philosophical Transactions of the Royal Society B*, 281(980), 277–294. <https://doi.org/10.1098/RSTB.1977.0140>
- Monteith, J. L. (1994). Validity of the correlation between intercepted radiation and biomass. *Agricultural and Forest Meteorology*, 68(3–4), 213–220. [https://doi.org/10.1016/0168-1923\(94\)90037-X](https://doi.org/10.1016/0168-1923(94)90037-X)
- Muluneh, M. G. (2021). Impact of climate change on biodiversity and food security: a global perspective—a review article. *Agriculture and Food Security*, 10(1), 1–25. <https://doi.org/10.1186/s40066-021-00318-5>
- Ojeda, H., Bigard, A., & Escudier, J. L. (2017). *De la vigne au vin: des créations variétales adaptées au changement climatique et résistant aux maladies cryptogamiques: 2/2 : Approche viticole pour des vins de type VDQA. Revue des Oenologues*, 44, 22–27.
- Osnato, M., Cota, I., Nebhnani, P., Cereijo, U., & Pelaz, S. (2022). Photoperiod Control of Plant Growth: Flowering Time Genes Beyond Flowering. *Frontiers in Plant Science*, 12(February), 1–20. <https://doi.org/10.3389/fpls.2021.805635>
- Ouyang, W., Gao, X., Hao, Z., Liu, H., Shi, Y., & Hao, F. (2017). Farmland shift due to climate warming and impacts on temporal-spatial distributions of water resources in a middle-high latitude agricultural watershed. *Journal of Hydrology*, 547, 156–167. <https://doi.org/10.1016/j.jhydrol.2017.01.050>

- Paradiso, R., & Proietti, S. (2022). Light-Quality Manipulation to Control Plant Growth and Photomorphogenesis in Greenhouse Horticulture: The State of the Art and the Opportunities of Modern LED Systems. *Journal of Plant Growth Regulation*, 41(2), 742–780. <https://doi.org/10.1007/s00344-021-10337-y>
- Pellegrino, A., Romieu, C., Rienth, M., & Torregrosa, L. (2019). The Microvine: A Versatile Plant Model to Boost Grapevine Studies in Physiology and Genetics. In T. Laurent, P. Anne, & R. Charles (Eds.), *Advances in Grape and Wine Biotechnology*: Vol. (1st editio, Issue, pp. 1–13). *IntechOpen*. <https://doi.org/10.5772/intechopen.86166>
- Pérez Asseff, J. M., Peña Salamanca, E. J., & Torres González, C. (2023). Efecto Del Nitrógeno Y La Irradianza En La Eficiencia Fotosintética Del Anamú Petiveria Alliacea (Phytolaccaceae). *Revista de La Academia Colombiana de Ciencias Exactas, Físicas y Naturales*, 31(118), 49–55. [https://doi.org/10.18257/raccefyn.31\(118\).2007.2306](https://doi.org/10.18257/raccefyn.31(118).2007.2306)
- Reich, P. B., Ellsworth, D. S., & Walters, M. B. (1998). Leaf structure (specific leaf area) modulates photosynthesis-nitrogen relations: Evidence from within and across species and functional groups. *Functional Ecology*, 12(6), 948–958. <https://doi.org/10.1046/j.1365-2435.1998.00274.x>
- Rienth, M., Jaquerod, A., Romieu, C., & Haute, C. (2016). *La microvine: un outil novateur pour la recherche et pour l'enseignement de la biologie de la vigne*. 48(2), 132–135.
- Sánchez-Gómez, R., Torregrosa, L., Zalacain, A., Ojeda, H., Bouckennooghe, V., Schneider, R., Alonso, G. L., & Salinas, M. R. (2018). The Microvine, a plant model to study the effect of vine-shoot extract on the accumulation of glycosylated aroma precursors in grapes. *Journal of the Science of Food and Agriculture*, 98(8), 3031–3040. <https://doi.org/10.1002/jsfa.8802>
- Savoi, S., Torregrosa, L., & Romieu, C. (2021). Transcripts switched off at the stop of phloem unloading highlight the energy efficiency of sugar import in the ripening V. vinifera fruit. *Horticulture Research*, 8(1). <https://doi.org/10.1038/s41438-021-00628-6>
- Shahood, R., Torregrosa, L., Savoi, S., & Romieu, C. (2020). First quantitative assessment of growth, sugar accumulation and malate breakdown in a single ripening berry. *Oeno One*, 54(4), 1077–1092. <https://doi.org/10.20870/OENO-ONE.2020.54.4.3787>
- Smith, A. M., & Stitt, M. (2007). Coordination of carbon supply and plant growth. *Plant, Cell and Environment*, 30(9), 1126–1149. <https://doi.org/10.1111/j.1365-3040.2007.01708.x>
- Taiz, L., Møller, I. M., Murphy, A., & Zeiger, E. (2015). Plant Physiology and Development. In *Plant Physiology and Development* (6th ed.). Sinauer Associates.
- Takahashi, S., & Badger, M. R. (2011). Photoprotection in plants: A new light on photosystem II damage. *Trends in Plant Science*, 16(1), 53–60. <https://doi.org/10.1016/j.tplants.2010.10.001>
- Taylor, J. R. (2020). Modeling the Potential Productivity of Urban Agriculture and Its Impacts on Soil Quality Through Experimental Research on Scale-Appropriate Systems. *Frontiers in Sustainable Food Systems*, 4(July), 1–18. <https://doi.org/10.3389/fsufs.2020.00089>
- Torregrosa, L., Rienth, M., Romieu, C., & Pellegrino, A. (2019). The microvine, a model for studies in grapevine physiology and genetics. *Oeno One*, 53(3), 373–391. <https://doi.org/10.20870/oeno-one.2019.53.3.2409>
- Velez-Ramirez, A. I., Van Ieperen, W., Vreugdenhil, D., & Millenaar, F. F. (2011). Plants under continuous light. *Trends in Plant Science*, 16(6), 310–318. <https://doi.org/10.1016/j.tplants.2011.02.003>
- Venkat, A., & Muneer, S. (2022). Role of Circadian Rhythms in Major Plant Metabolic and Signaling Pathways. *Frontiers in Plant Science*, 13(April), 1–11. <https://doi.org/10.3389/fpls.2022.836244>
- Villalobos-González, L., Alarcón, N., Bastías, R., Pérez, C., Sanz, R., Peña-Neira, Á., & Pastenes, C. (2022). Correction: Villalobos-González et al. Photoprotection Is Achieved by Photorespiration and Modification of the Leaf Incident Light, and Their Extent Is Modulated by the Stomatal Sensitivity to Water Deficit in Grapevines, (Plants, (2022), 11, (1050), 10.3. *Plants*, 11(16). <https://doi.org/10.3390/plants11162096>
- Westgeest, A. J., Dauzat, M., Simonneau, T., & Pantin, F. (2023). Leaf starch metabolism sets the phase of stomatal rhythm. *Plant Cell*, 35(9), 3444–3469. <https://doi.org/10.1093/plcell/koad158>
- Zeeman, S. C., Smith, S. M., & Smith, A. M. (2007). The diurnal metabolism of leaf starch. *Biochemical Journal*, 401(1), 13–28. <https://doi.org/10.1042/BJ20061393>
- Zhang, X., Yuan, H., Guan, L., Wang, X., Wang, Y., Jiang, Z., Cao, L., & Zhang, X. (2019). Influence of Photoperiods on Microalgae Biofilm: *Energies*, 12, 3724. <https://doi.org/10.3390/en12193724>